Correlated disorder induced anomalous transport in magnetically doped topological insulators

Takuya Okugawa [1], Tanay Nag [1,*] and Dante M. Kennes [1,2,†]
[1] *Institut für Theorie der Statistischen Physik, RWTH Aachen, 52056 Aachen, Germany and JARA - Fundamentals of Future Information Technology*
[2] *Max Planck Institute for the Structure and Dynamics of Matter, Center for Free Electron Laser Science, 22761 Hamburg, Germany*

(Received 15 March 2022; revised 3 June 2022; accepted 5 July 2022; published 18 July 2022)

We examine the transport properties of magnetically doped topological insulator (TI) thin films subject to correlated nonmagnetic disorder. For the disorder we choose a quasiperiodic potential with a random phase. We restrict the disorder to a central region, which is coupled to two leads in a clean quantum spin Hall insulator (QSHI) state and concentrate on different orientations of the quasiperiodicity in the two-dimensional central region. In the case of a diagonally oriented or purely longitudinal quasiperiodicity we find different topological Anderson insulator (TAI) phases, with a quantum anomalous Hall insulator (QAHI), a quantum spin Chern insulator (QSCI), or a QSHI phase being realized before the Anderson insulation takes over at large disorder strength. Quantized transport from extended bulk states is found for diagonal quasiperiodicity in addition to the above TAI phases that are also observed for the case of uncorrelated disorder. For a purely transverse orientation of the quasiperiodicity the emerging QSHI and QSCI phases persist to arbitrarily strong disorder potential. These topological phase transitions (except to the Anderson insulator phase) can be understood from a self consistent Born approximation.

DOI: 10.1103/PhysRevB.106.045417

I. INTRODUCTION

In recent years various noninteracting quantum Hall phases such as, the quantum anomalous Hall insulator (QAHI) [1,2], the quantum spin Hall insulator (QSHI) [3–5], as well as Weyl and Dirac semimetals [6–8] have been identified. The QSHI phases have been proposed theoretically [9,10] as well as observed experimentally [11,12] in nonmagnetic materials for example, HgTe and Bi_2Te_3. Interestingly, the QSHI turns into a QAHI, harbouring chiral edge states, when time reversal symmetry (TRS) is broken [7,13–18]. This can be achieved by magnetic doping [19,20], exchange field [21,22], and staggered magnetic flux [23], and was recently experimentally realized [24–34].

Remarkably, the QSHI phases are robust against weak nonmagnetic disorder while moderate disorder can induce a topological phase, called a topological Anderson insulator (TAI), even if the clean system remains a normal insulator (NI) [35–37]. The disorder results in a negative mass term for the band inversion as captured by the self consistent Born approximation (SCBA). Importantly, weak magnetic disorder is shown to stabilize the QAHI phase while the AI phase emerges for substantially strong disorder [38–49]. However, nonmagnetic disorder, originating from the spatial inhomogeneities constitutes an important factor in experiments as well [31,46,47,50–52] and has attracted recent attention [53–59]. The nature of the various TAI phases also depend on the types of disorder such as, site versus bond disorders [60].

Interestingly, the topological phase transitions (TPTs) in the presence of both nonmagnetic correlated disorder, caused by quasiperiodic Aubry-André-Harper potential [61] in the two dimensional (2D) plane, and the magnetic exchange field remain uncharted so far while the effect of on-site random disorder [58], correlated disorder [62,63], and magnetic disorder [41,42] are investigated separately. Also, the random disorder effects on topological Penrose-type quasicrystal systems [64] and magnetic Weyl semimetal in the presence of intra and inter-orbital disorder [65] have been already studied. In particular, we answer the following question, which is experimentally relevant as well [25,26]: How can we understand the rich interplay between magnetism and orientation of correlated disorder in the 2D plane by examining the topological phase diagram? The existence of a mobility edge in one-dimensional (1D) quasiperiodic systems [66–71] further motivates us to explore its connection with the edge transport in 2D topological systems.

In this paper, we consider Bi_2Te_3 thin film in the presence of magnetic exchange field and correlated disorder (here, chosen as a quasiperiodic potential with random phase), coupled to two semi-infinite clean nonmagnetic leads in the QSHI phase, to investigate the conductance through the former. The disorder, depending upon its orientation (see Fig. 1), can mediate a series of TPTs as observed in the rich phase diagrams where the system transits through a number of phases such as, NI, QAHI, QSHI, quantum spin Chern insulator (QSCI), and AI phases. The diagonal quasiperiodic case, called isotropic in the following, surprisingly yields quantized conductance

*tnag@physik.rwth-aachen.de
†dante.kennes@rwth-aachen.de

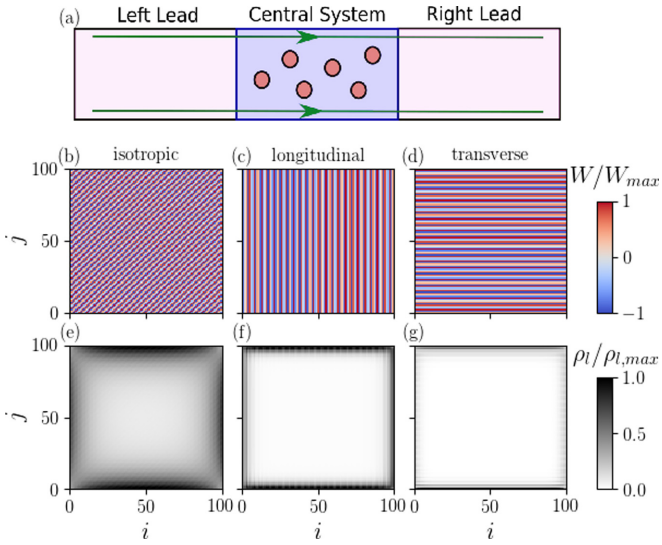

FIG. 1. The studied setup is demonstrated in (a). The spatial representation of quasiperiodic potential $\epsilon_r = \cos(2\pi\eta r)$ and disorder averaged local density of states from the retarded Greens function of the central system are shown for isotropic [(b),(e)]; longitudinal [(c),(f)]; and transverse [(d),(g)] cases. Here, r represents the location of lattice sites on the 2D square lattice. We choose $gM = 30$ and $W = 350\,\text{meV}$ to depict edge modes at $j = 1,\ 100$ for the QAHI phase in [(e)–(g)].

from the extended bulk states beside the TAI (QAHI, QSHI, and QSCI) phases with quantized edge transport (see Fig. 2). For anisotropic longitudinal [transverse] quasiperiodicity, the QSCI phase gets remarkably suppressed [extended] when the exchange field and disorder amplitude increase (see Fig. 3) [see Fig. 4]. The TPTs in the above cases are successfully captured by the sign change of renormalized mass term computed from SCBA.

II. MODEL AND METHOD

We start with a model of three quintuple layers of (Bi, Sb)$_2$Te$_3$ given by [9,72,79]

$$H_0(\boldsymbol{k}) = \boldsymbol{N}\cdot\boldsymbol{\Gamma} = \sum_{i=1}^{3} N_i\Gamma_i \tag{1}$$

where $N_1 = v_F\sin(k_y a)/a$, $N_2 = -v_F\sin(k_x a)/a$, $N_3 = m(\boldsymbol{k}) = m_0 + 2B[2-\cos(k_x a)-\cos(k_y a)]/a^2$, and $\Gamma_1 = \tau_x\sigma_0$, $\Gamma_2 = \tau_y\sigma_z$, and $\Gamma_3 = \tau_z\sigma_0$. We note that $\boldsymbol{\tau}$ and $\boldsymbol{\sigma}$ represent orbital and spin degrees of freedom. Here, v_F (a) denotes the Fermi velocity (lattice spacing). A ferromagnetic order in the above topological insulator (TI) thin film can be induced by magnetic doping with Cr or Fe atoms [25,27,72]. Such a TRS broken TI can be modeled as $H(\boldsymbol{k}) = H_0(\boldsymbol{k}) + gM\tau_z\sigma_z$ where g represents the Landé g factor and M is the magnetic exchange field. The Hamiltonian thus reads in the block-diagonal form [24]:

$$H(\boldsymbol{k}) = \begin{pmatrix} H_u(\boldsymbol{k}) & 0 \\ 0 & H_l(\boldsymbol{k}) \end{pmatrix}, \tag{2}$$

where the upper and lower block Hamiltonian $H_{u,l}(\boldsymbol{k}) = N_{\mp}\sigma_{+} + N_{\pm}\sigma_{-} + m_{u,l}(\boldsymbol{k})\sigma_z$ with $N_{\pm} = N_1 \pm iN_2$, $\sigma_{\pm} = (\sigma_x \pm i\sigma_y)/2$ and $m_{u,l}(\boldsymbol{k}) = N_3 \pm gM$.

We study the effect of an on-site nonmagnetic impurity potential on the central magnetic TI [Eq. (2)] of dimension $L_x \times L_y$, which is coupled to semi-infinite QSHI leads [Eq. (1)]. The setup is shown in Fig. 1(a). We model the impurity potential by a quasiperiodic potential with random phase $\epsilon_{i,j} = W\cos[2\pi\eta(i\alpha + j\beta) + \phi]/2$, where W denotes the amplitude of the potential, i.e., disorder strength, ϕ is an offset chosen from a uniform random distribution between [0,2 π), and $\eta = (\sqrt{5}-1)/2$ is an irrational number. The disorder correlation function takes the form $C_{m,n} = \langle\epsilon_{i,j}\epsilon_{i+m,j+n}\rangle = W^2\cos[2\pi\eta(m\alpha + n\beta)]/8$. Owing to the finite value of $C_{m,n}$ for quasiperiodic potential with random phase, unlike the random potential with $C_{m,n} = \delta_{n,0}\delta_{m,0}$, we refer to $\epsilon_{i,j}$ as correlated disorder. The real space Hamiltonian for the central system and the leads are given by $H_{\text{CS}}(m_0, M, W) = \sum_{rr'}[\mathcal{H}_{rr'}(m_0, M) + \epsilon_r\delta_{r,r'}]C_r^{\dagger}C_{r'}$ and $H_{L,R}(m_0) = H_{\text{CS}}(-|m_0|, M = 0, W = 0)$, respectively, where $\mathcal{H}_{rr'}(m_0, M)$ is obtained from a Fourier transformation of $H(\boldsymbol{k})$ in Eq. (2) where r represents the location of lattice sites on the 2D square lattice. The annihilation (creation) operator C_r ($C_r^{\dagger}$) consists of a two-orbital and a spin-1/2 degrees of freedom. We note that on-site disorder breaks the particle-hole symmetry.

Generally, $\alpha = \beta = 1$ refers to the 2D isotropic (diagonally oriented) quasiperiodicity. We also consider purely longitudinal (transverse) quasiperiodicity only along x (y) direction choosing $\alpha = 1,\ \beta = 0$ ($\alpha = 0,\ \beta = 1$). The spatial configurations of these disorder potentials are demonstrated in Figs. 1(b), 1(c), and 1(d) for $\phi = 0$. Here, we consider a thickness of three quintuple layers such that the model becomes trivial in the clean and undoped limit with appropriate material parameters: $v_F = 3.07\,\text{eV Å}$, $m_0 = 44\,\text{meV}$, $B = 37.3\,\text{eV Å}^2$ [72], and $a = 20$ Å [58]. We compute the disorder averaged conductance G (in units of e^2/h) for the central region and the corresponding standard deviation δG (in units of e^2/h), following the Landauer-Büttiker formalism [73,74] with recursive Green's function technique [58,75–77], as a function of both disorder strength W and exchange field gM (see Figs. 2–4). The QSHI and QSCI phases both are identified by quantized conductance $G = 2$ (green) while the former [latter] appears in the absence [presence] of exchange field. The QAHI phases are characterized by quantized conductance $G = 1$ (orange).

We also analyze the emergence of disorder mediated TPTs using the SCBA [36]. Importantly, TAI phases appear when the renormalized topological mass $\overline{m} = m + \delta m$ becomes negative $\overline{m} < 0$ as well as the renormalized chemical potential $\overline{E}_F = E_F + \delta\mu$ lies inside the band gap $|\overline{E}_F| < -\bar{m}$. Exploiting the block diagonal form of the Hamiltonian [Eq. (2)], we can decompose the self-energy into upper and lower blocks $\Sigma_{u,l} = \Sigma_0^{u,l}\sigma_0 + \Sigma_x^{u,l}\sigma_x + \Sigma_y^{u,l}\sigma_y + \Sigma_z^{u,l}\sigma_z$. The correction terms, caused by the disorder, are thus found to be $\delta m_{u,l} = \text{Re}[\Sigma_z^{u,l}]$ and $\delta\mu_{u,l} = -\text{Re}[\Sigma_0^{u,l}]$. The self-energy can be expressed through self-consistent equations by incorporating $C(\boldsymbol{k})$, i.e., Fourier transform of the disorder correlation function $C_{m,n}$, as follows

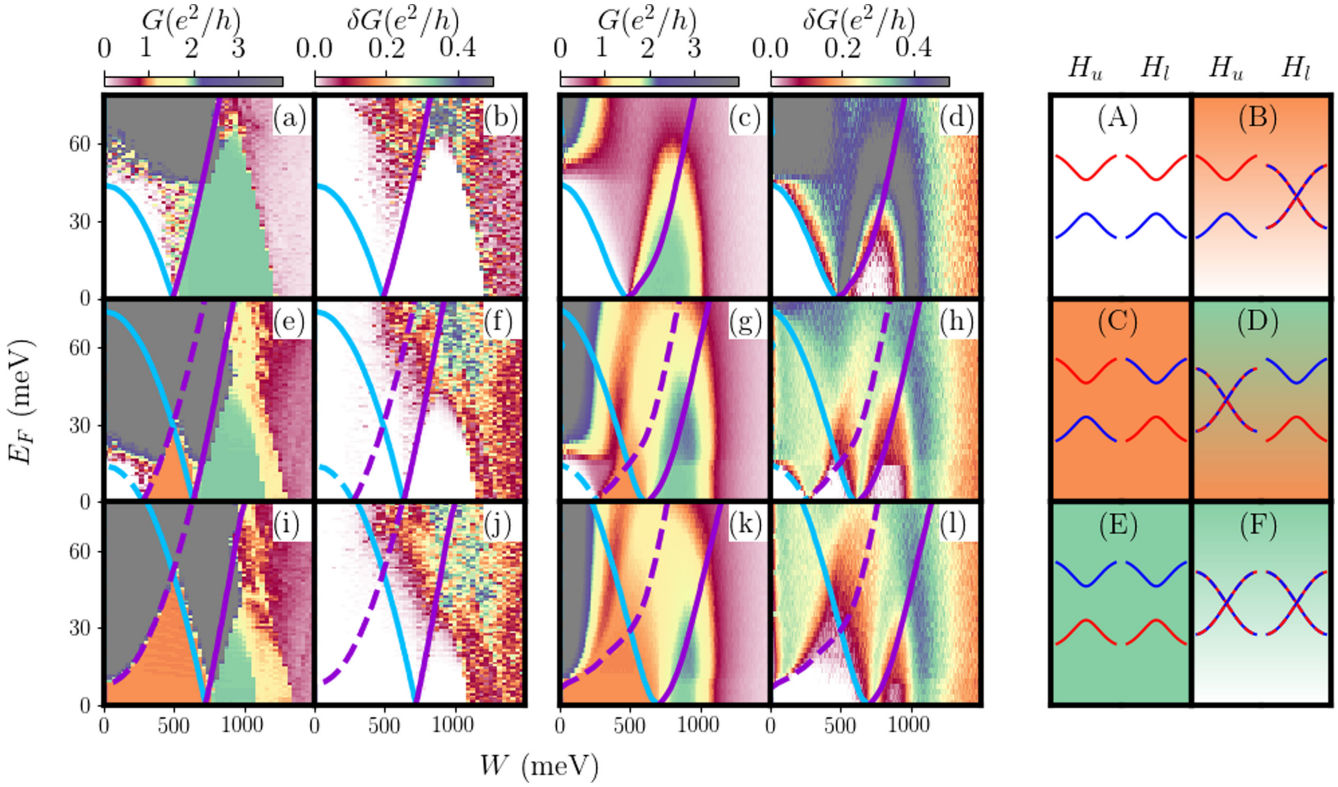

FIG. 2. (a), (e), and (i) [(c), (g), and (k)] depict the conductance G with $gM = 0$, 30, and 52 meV, respectively, for isotropic correlated disorder $\epsilon_r = W\cos(2\pi\eta r + \phi)/2$ with $\alpha = \beta = 1$ (uncorrelated random disorder $\epsilon_r \in [-W/2, W/2]$ [58]). The corresponding standard deviation δG are shown for isotropic correlated [uncorrelated random] disorder in (b), (f), and (j) [(d), (h), and (l)]. We consider a central system $H_{\rm CS}(m_0, M, W)$ of dimension $L_x \times L_y = 400a \times 100a$ and $400a \times 200a$, respectively, for zero and nonzero values of gM. The solid and dashed [blue and purple] lines trace out the phase boundaries associated with $H_u(\boldsymbol{k})$ and $H_l(\boldsymbol{k})$ [$|\overline{E}_F^{u,l}| = \overline{m}_0^{u,l}$ and $|\overline{E}_F^{u,l}| = -\overline{m}_0^{u,l}$], respectively, according to the SCBA. The cartoon pictures (A)–(F), depict the evolution of the band gap for topological (red valence and blue conduction bands in the uniform orange and green background) and trivial (blue valence and red conduction bands in the white background) phases for $H_{u,l}(\boldsymbol{k})$ separately.

[62,63,78,79]:

$$\Sigma_{u,l} = \int d\boldsymbol{k}\, C(\boldsymbol{k})\,(E_F + i\zeta - H_{u,l}(\boldsymbol{k}) - \Sigma_{u,l})^{-1} = W^2(\Sigma^+_{u,l} + \Sigma^-_{u,l})/16 \quad (3)$$

with $\Sigma^{\pm}_{u,l} = (E_F + i\zeta - H_{u,l}(\pm\alpha Q, \pm\beta Q) - \Sigma_{u,l})^{-1}$, $Q = 2\pi\eta$ and $\zeta \to 0$. The phase boundaries can be determined by $|\overline{E}_F^{u,l}| = -\overline{m}_0^{u,l}$ for $\overline{m}_0^{u,l} < 0$ and $|\overline{E}_F^{u,l}| = \overline{m}_0^{u,l}$ for $\overline{m}_0^{u,l} > 0$ segregating the TAI phases with quantized $G \neq 0$ from the trivial phases with nonquantized G. Note that the SCBA fails to detect the TPTs to an AI phase for strong disorder $W > \mathcal{O}(B/a^2, v_F/a)$.

III. RESULTS

We start our discussion on TPTs induced by the correlated disorder with Fig. 2 where we consider the isotropic quasiperiodicity, i.e., $\alpha = \beta = 1$ [see Fig. 1(a)] and compare to the random disorder case [58]. The bulk gap Δ of the central system can be read off by the Fermi energy E_F at which the quantized conductance $G = 0$, 1, and 2 (accompanied by $\delta G = 0$) can either change to a nonquantized value with $\delta G \neq 0$ or a quantized value with $G > 2$. The later phase with $G > 2$ is exclusively observed for the case of correlated disorder, which stems from extended bulk modes lying well above the trivial and topological gap. The thin film is in the NI phase for $\Delta = m_0 = 44$ meV in the clean nonmagnetic case [see Fig. 2(a)]. With increasing disorder strength regardless of whether the disorder is correlated or uncorrelated, the trivial gap reduces and eventually the gap becomes topological at $(W, E_F) \approx (500\text{ meV}, 0\text{ meV})$, i.e., $\Delta < 0$ due to band inversion. At this point the thin film enters into a QSHI phase with quantized $G = 2$. The QSHI phase has a maximal gap at $W \approx 900$ meV and for larger disorder W rapidly turns into an AI. Upon including a magnetic field $gM = 30$ meV as shown in Fig. 2(e), the trivial gap Δ reduces to 14 meV in the clean limit. The trivial system now first enters into a QAHI with quantized $G = 1$ upon inclusion of disorder, followed by a QSCI phase with quantized $G = 2$ and eventually an AI phase takes over for strong disorder. Upon increasing the magnetic field to $gM = 52$ meV, as shown in Fig. 2(i), the system already resides in the QAHI phase, with topological gap $|\Delta| = 8$ meV, even in the clean limit. For increasing disorder W, the system similarly traverses through a series of QAHI $\to$ QSCI $\to$ AI phases. However, the size of the QSCI (QAHI) phase decreases (increases) significantly for $gM = 52$ meV as compared to that of $gM = 30$ meV.

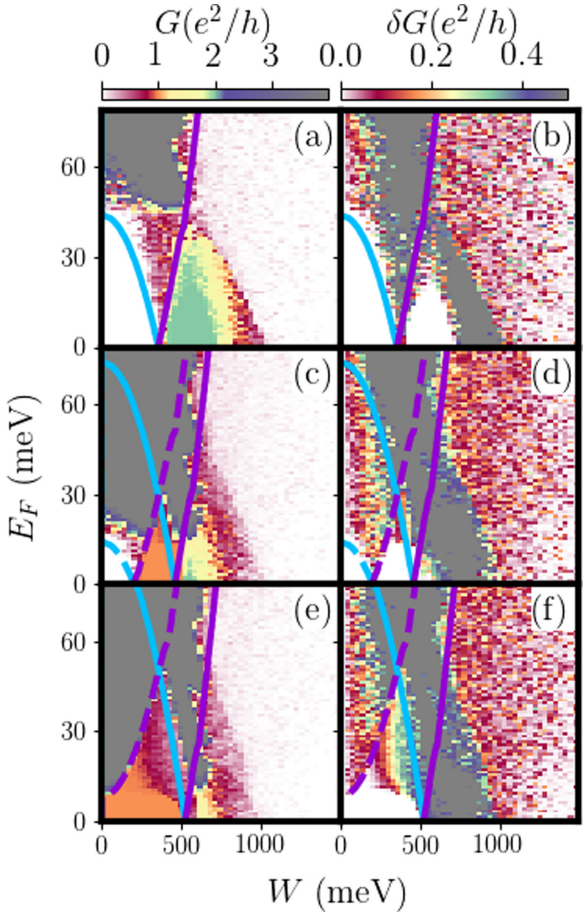

FIG. 3. We investigate the longitudinal quasiperiodicity, $\alpha = 1$ and $\beta = 0$ for the same set of parameters as Fig. 2. The size of the QSHI (QSCI) phase for zero (nonzero) values of gM reduces as compared to the Figs. 2(a) and 2(e).

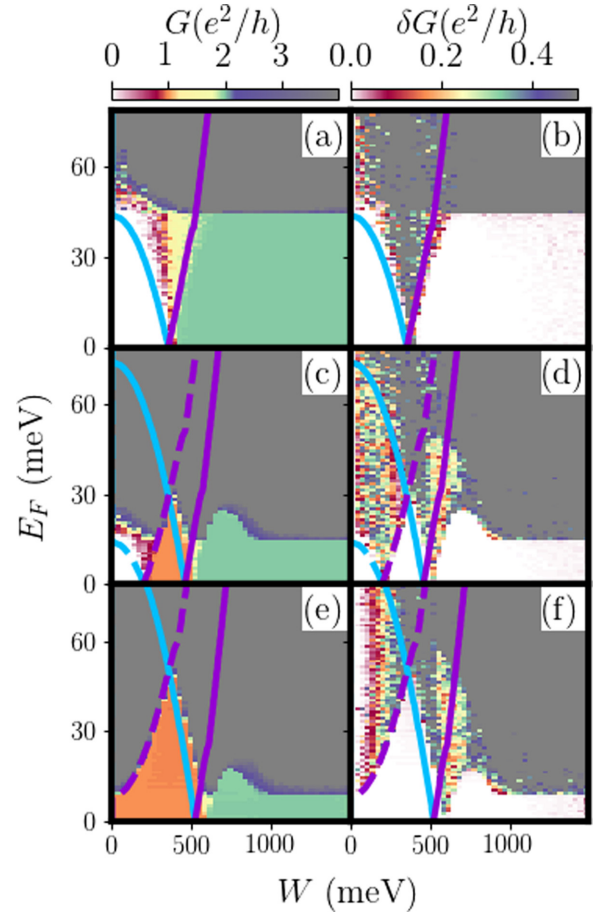

FIG. 4. We investigate the transverse quasiperiodicity, $\alpha = 0$ and $\beta = 1$ for the same set of parameters as Fig. 2. The QSHI (QSCI) phase remains stable even at strong disorder unlike in the other two cases shown in Figs. 2 and 3.

The different TPTs except the transition to the AI phase at large disorder are well captured by the SCBA as indicated by the lines in Fig. 2. The evolution of the bulk gap for the central system in various phases and their boundaries are schematically demonstrated in Figs. 2(A)–2(F). All these above features, obtained for correlated disorder, are qualitatively similar to random disorder. However, the correlated disorder is found to stabilize the TAI phases more clearly than random disorder as evident from the standard deviation δG profiles [see Figs. 2(b), 2(d), 2(f), 2(h), 2(j), and 2(l)].

For longitudinal quasiperiodicity $\alpha = 1$ and $\beta = 0$ [see Fig. 1(b)] we find a qualitatively similar picture, as shown in Fig. 3, compared to the previous isotropic case. Interestingly, the marked differences are that the quantized transport from the bulk mode as well as the QSCI phase at larger magnetic fields gM are absent in the present case. The latter is due to the reservoir effect: When the topological gap of the lead is less than or comparable to the gap of the central system, a hybridization of the edge modes in the central system with the bulk modes in the leads may occur. The reservoir effect is analyzed in more detail in the Sec. II in the Supplemental Material (SM) [79].

Next we analyze transverse quasiperiodicity along y direction, i.e., perpendicular to the transport direction, with $\alpha = 0$ and $\beta = 1$ [see Fig. 1(c)]. Contrary to the above cases, the QSHI and QSCI phases continue to exist with a topological gap $\Delta < 0$ even for strong disorder $W > 1000$ meV irrespective of the values of exchange field as shown in Figs. 4(a), 4(c), and 4(e). This effect unique to the case of transverse quasiperiodicity can be captured within a simple SCBA approach. It is noteworthy that the phase transition boundaries, evaluated by SCBA, are exactly the same in Figs. 3 and 4. This is due to the underlying C_4 symmetry of the clean central system. The above crystalline symmetry further ensures that the phase diagram for longitudinal (Fig. 3) and transverse (Fig. 4) quasiperiodicities would be interchanged once the leads are connected to the top and bottom instead of the left and right of the central system. The results only depend on the relative orientation of the quasiperiodicity with regard to the transport direction.

IV. DISCUSSIONS

It is evident from the above investigations that the upper and lower block of the Hamiltonian in Eq. (2), can be selectively made topological under the appropriate orientations of correlated disorder. With increasing disorder W, the lower block becomes topological first followed by the upper block.

As long as the direction of the magnetic field is not altered, the above feature is observed in all the cases (flipping the magnetic field flips upper and lower block). We note that the individual phases for $E_F > 0$ would also symmetrically appear for $E_F < 0$ owing to the emergent spectral symmetry of the system under $W \to -W$ (see Sec. IV in the SM for more discussion) [58,79].

The quasiperiodicity generically introduces mobility edges such that there exist extended bulk states within an energy interval between $[E_-, E_+]$ in the middle of the single particle spectrum around zero energy (see Sec. V in the SM [79] for more discussion). One expects these states to participate in the electron transport through the central disordered system above its bulk gap Δ provided $|\Delta| < |E_+ - E_-|$. For the isotropic quasiperiodicity, this mechanism of bulk transport might lead to the quantized conductance with $G > 2$ and $\delta G \to 0$ even though $\overline{m}_0^{u,l} > 0$ [see Figs. 2(a), 2(e), and 2(i)]. These regions appear just outside the NI and TAI phases when $E_- < E_F < E_+$ and $|E_F| > |\Delta|$, in marked contrast to the random disorder case. The universality classes of the TPTs between the TAI and non-TAI phases, [62,63,80–82] reported here are left for future research.

On the other hand, for anisotropic quasiperiodicities, the mobility edge energy interval $|E_+ - E_-|$ for the extended bulk states shrinks significantly resulting in the suppression of quantized transport from the bulk states lying above $|\Delta|$. This could be the reason why nonquantized bulk conductance with $G > 2$ and $\delta G > 0$ for longitudinal and transverse quasiperiodicities is observed. The edge transport along x direction is severely (minimally) influenced for longitudinal (transverse) quasiperiodicity as the midgap conducting edge modes can (can not) become localized, which are otherwise delocalized along the transport direction at $y = 1, L_y$ [see Figs. 1(e)–1(g)]. Combining these insights one notes that the TAI phase diagram for isotropic quasiperiodicity is an admixture of the anisotropic quasiperiodicities along longitudinal and transverse directions.

Our findings suggest that in terms of the current transport, the AI phase does not emerge for the transverse quasiperiodic case unlike to the remaining cases. In the strong disorder regime, localized states reside in the interior bulk of the central system. For the 1D quasiperiodicity, such localization is expected to occur only over the 1D line of lattice sites on which the quasiperiodicity is embedded. This further indicates that longitudinal quasiperiodicity leads to spatially separated localized states through which the transport current can not propagate. The same is also true for diagonal quasiperiodicity. On the other hand, for transverse quasiperiodicity, such localization along the y direction essentially allows the current flow.

Our study is potentially relevant to model the experimental findings on QAHI phases in magnetic TIs [25,26,31,83–85]. Besides solid-state systems, TIs are also realized for ultracold atomic gases in optical lattices [86–91]. To be specific, The Su-Schrieffer-Heeger model [92] has already been implemented in optical lattice [93]. Furthermore, the quasiperiodic potential has been proposed [94] and implemented [95] in optical lattices. The optical laser speckle potential could be engineered to introduce the correlated disorder of the type discussed here [96,97]. In the light of the above considerations, we believe that TPTs induced by the interplay between the correlated disorder and magnetism can be investigated with ultracold atoms.

ACKNOWLEDGMENTS

This work was supported by the Deutsche Forschungsgemeinschaft (DFG, German Research Foundation) via RTG 1995 and Germanys Excellence Strategy - Cluster of Excellence Matter and Light for Quantum Computing (ML4Q) Grant No. EXC 2004/1 - 390534769. Simulations were performed with computing resources granted by RWTH Aachen University under Project No. rwth0857. We acknowledge support from the Max Planck-New York City Center for Non-Equilibrium Quantum Phenomena.

T.O. performed the calculations. T.N. conceived the project. T.N. and D.M.K. supervised the project. All the authors contributed to the manuscript.

[1] F. D. M. Haldane, Phys. Rev. Lett. **61**, 2015 (1988).
[2] M. Onoda and N. Nagaosa, Phys. Rev. Lett. **90**, 206601 (2003).
[3] C. L. Kane and E. J. Mele, Phys. Rev. Lett. **95**, 226801 (2005).
[4] D. N. Sheng, Z. Y. Weng, L. Sheng, and F. D. M. Haldane, Phys. Rev. Lett. **97**, 036808 (2006).
[5] B. A. Bernevig and S.-C. Zhang, Phys. Rev. Lett. **96**, 106802 (2006).
[6] M. Z. Hasan and C. L. Kane, Rev. Mod. Phys. **82**, 3045 (2010).
[7] C.-X. Liu, S.-C. Zhang, and X.-L. Qi, Annu. Rev. Condens. Matter Phys. **7**, 301 (2016).
[8] N. P. Armitage, E. J. Mele, and A. Vishwanath, Rev. Mod. Phys. **90**, 015001 (2018).
[9] B. A. Bernevig, T. L. Hughes, and S.-C. Zhang, Science **314**, 1757 (2006).
[10] H. Zhang, C.-X. Liu, X.-L. Qi, X. Dai, Z. Fang, and S.-C. Zhang, Nat. Phys. **5**, 438 (2009).
[11] M. König, S. Wiedmann, C. Brüne, A. Roth, H. Buhmann, L. W. Molenkamp, X.-L. Qi, and S.-C. Zhang, Science **318**, 766 (2007).
[12] A. Roth, C. Brüne, H. Buhmann, L. W. Molenkamp, J. Maciejko, X.-L. Qi, and S.-C. Zhang, Science **325**, 294 (2009).
[13] R. S. K. Mong, A. M. Essin, and J. E. Moore, Phys. Rev. B **81**, 245209 (2010).
[14] M. M. Otrokov, I. I. Klimovskikh, H. Bentmann, D. Estyunin, A. Zeugner, Z. S. Aliev, S. Gaß, A. Wolter, A. Koroleva, A. M. Shikin *et al.*, Nature (London) **576**, 416 (2019).
[15] J. Li, Y. Li, S. Du, Z. Wang, B.-L. Gu, S.-C. Zhang, K. He, W. Duan, and Y. Xu, Sci. Adv. **5**, eaaw5685 (2019).
[16] P. Tang, Q. Zhou, G. Xu, and S.-C. Zhang, Nat. Phys. **12**, 1100 (2016).
[17] K. He, Y. Wang, and Q.-K. Xue, Annu. Rev. Condens. Matter Phys. **9**, 329 (2018).

[18] S. Saha, T. Nag, and S. Mandal, Phys. Rev. B **103**, 235154 (2021).

[19] C.-X. Liu, X.-L. Qi, X. Dai, Z. Fang, and S.-C. Zhang, Phys. Rev. Lett. **101**, 146802 (2008).

[20] H. Li, L. Sheng, R. Shen, L. B. Shao, B. Wang, D. N. Sheng, and D. Y. Xing, Phys. Rev. Lett. **110**, 266802 (2013).

[21] Z. Qiao, S. A. Yang, W. Feng, W.-K. Tse, J. Ding, Y. Yao, J. Wang, and Q. Niu, Phys. Rev. B **82**, 161414(R) (2010).

[22] Y. Yang, Z. Xu, L. Sheng, B. Wang, D. Y. Xing, and D. N. Sheng, Phys. Rev. Lett. **107**, 066602 (2011).

[23] W. Luo, D. Shao, M.-X. Deng, W. Deng, and L. Sheng, Sci. Rep. **7**, 43049 (2017).

[24] R. Yu, W. Zhang, H.-J. Zhang, S.-C. Zhang, X. Dai, and Z. Fang, Science **329**, 61 (2010).

[25] C.-Z. Chang, J. Zhang, X. Feng, J. Shen, Z. Zhang, M. Guo, K. Li, Y. Ou, P. Wei, L.-L. Wang *et al.*, Science **340**, 167 (2013).

[26] J. G. Checkelsky, R. Yoshimi, A. Tsukazaki, K. S. Takahashi, Y. Kozuka, J. Falson, M. Kawasaki, and Y. Tokura, Nat. Phys. **10**, 731 (2014).

[27] C.-Z. Chang, W. Zhao, D. Y. Kim, H. Zhang, B. A. Assaf, D. Heiman, S.-C. Zhang, C. Liu, M. H. Chan, and J. S. Moodera, Nat. Mater. **14**, 473 (2015).

[28] Y. Feng, X. Feng, Y. Ou, J. Wang, C. Liu, L. Zhang, D. Zhao, G. Jiang, S.-C. Zhang, K. He, X. Ma, Q.-K. Xue, and Y. Wang, Phys. Rev. Lett. **115**, 126801 (2015).

[29] X. Kou, S.-T. Guo, Y. Fan, L. Pan, M. Lang, Y. Jiang, Q. Shao, T. Nie, K. Murata, J. Tang, Y. Wang, L. He, T.-K. Lee, W.-L. Lee, and K. L. Wang, Phys. Rev. Lett. **113**, 137201 (2014).

[30] A. J. Bestwick, E. J. Fox, X. Kou, L. Pan, K. L. Wang, and D. Goldhaber-Gordon, Phys. Rev. Lett. **114**, 187201 (2015).

[31] C.-Z. Chang, W. Zhao, J. Li, J. K. Jain, C. Liu, J. S. Moodera, and M. H. W. Chan, Phys. Rev. Lett. **117**, 126802 (2016).

[32] K. Yasuda, M. Mogi, R. Yoshimi, A. Tsukazaki, K. S. Takahashi, M. Kawasaki, F. Kagawa, and Y. Tokura, Science **358**, 1311 (2017).

[33] A. L. Sharpe, E. J. Fox, A. W. Barnard, J. Finney, K. Watanabe, T. Taniguchi, M. Kastner, and D. Goldhaber-Gordon, Science **365**, 605 (2019).

[34] M. Serlin, C. Tschirhart, H. Polshyn, Y. Zhang, J. Zhu, K. Watanabe, T. Taniguchi, L. Balents, and A. Young, Science **367**, 900 (2020).

[35] J. Li, R.-L. Chu, J. K. Jain, and S.-Q. Shen, Phys. Rev. Lett. **102**, 136806 (2009).

[36] C. W. Groth, M. Wimmer, A. R. Akhmerov, J. Tworzydło, and C. W. J. Beenakker, Phys. Rev. Lett. **103**, 196805 (2009).

[37] H.-M. Guo, G. Rosenberg, G. Refael, and M. Franz, Phys. Rev. Lett. **105**, 216601 (2010).

[38] K. Nomura and N. Nagaosa, Phys. Rev. Lett. **106**, 166802 (2011).

[39] H.-Z. Lu, J. Shi, and S.-Q. Shen, Phys. Rev. Lett. **107**, 076801 (2011).

[40] Z. Qiao, Y. Han, L. Zhang, K. Wang, X. Deng, H. Jiang, S. A. Yang, J. Wang, and Q. Niu, Phys. Rev. Lett. **117**, 056802 (2016).

[41] C.-Z. Chen, H. Liu, and X. C. Xie, Phys. Rev. Lett. **122**, 026601 (2019).

[42] A. Haim, R. Ilan, and J. Alicea, Phys. Rev. Lett. **123**, 046801 (2019).

[43] Y. Xing, F. Xu, K. T. Cheung, Q.-f. Sun, J. Wang, and Y. Yao, New J. Phys. **20**, 043011 (2018).

[44] J. Wang, B. Lian, and S.-C. Zhang, Phys. Rev. B **89**, 085106 (2014).

[45] A. C. Keser, R. Raimondi, and D. Culcer, Phys. Rev. Lett. **123**, 126603 (2019).

[46] W. Wang, Y. Ou, C. Liu, Y. Wang, K. He, Q.-K. Xue, and W. Wu, Nat. Phys. **14**, 791 (2018).

[47] I. Lee, C. K. Kim, J. Lee, S. J. Billinge, R. Zhong, J. A. Schneeloch, T. Liu, T. Valla, J. M. Tranquada, G. Gu *et al.*, Proc. Natl. Acad. Sci. USA **112**, 1316 (2015).

[48] E. O. Lachman, A. F. Young, A. Richardella, J. Cuppens, H. Naren, Y. Anahory, A. Y. Meltzer, A. Kandala, S. Kempinger, Y. Myasoedov *et al.*, Sci. Adv. **1**, e1500740 (2015).

[49] X. Kou, L. Pan, J. Wang, Y. Fan, E. S. Choi, W.-L. Lee, T. Nie, K. Murata, Q. Shao, S.-C. Zhang *et al.*, Nat. Commun. **6**, 8474 (2015).

[50] Y. Yuan, X. Wang, H. Li, J. Li, Y. Ji, Z. Hao, Y. Wu, K. He, Y. Wang, Y. Xu, W. Duan, W. Li, and Q.-K. Xue, Nano Lett. **20**, 3271 (2020).

[51] C. Chen, M. Teague, L. He, X. Kou, M. Lang, W. Fan, N. Woodward, K. Wang, and N. Yeh, New J. Phys. **17**, 113042 (2015).

[52] J. Liao, Y. Ou, X. Feng, S. Yang, C. Lin, W. Yang, K. Wu, K. He, X. Ma, Q.-K. Xue, and Y. Li, Phys. Rev. Lett. **114**, 216601 (2015).

[53] Y. Xing, L. Zhang, and J. Wang, Phys. Rev. B **84**, 035110 (2011).

[54] E. Prodan, Phys. Rev. B **83**, 195119 (2011).

[55] A. Yamakage, K. Nomura, K.-I. Imura, and Y. Kuramoto, J. Phys. Soc. Jpn. **80**, 053703 (2011).

[56] Y.-Y. Zhang, R.-L. Chu, F.-C. Zhang, and S.-Q. Shen, Phys. Rev. B **85**, 035107 (2012).

[57] D. Xu, J. Qi, J. Liu, V. Sacksteder, X. C. Xie, and H. Jiang, Phys. Rev. B **85**, 195140 (2012).

[58] T. Okugawa, P. Tang, A. Rubio, and D. M. Kennes, Phys. Rev. B **102**, 201405(R) (2020).

[59] Z.-Q. Zhang, C.-Z. Chen, Y. Wu, H. Jiang, J. Liu, Q.-f. Sun, and X. C. Xie, Phys. Rev. B **103**, 075434 (2021).

[60] J. Song, H. Liu, H. Jiang, Q.-f. Sun, and X. C. Xie, Phys. Rev. B **85**, 195125 (2012).

[61] S. Aubry and G. André, Ann. Israel. Phys. Soc. **3**, 133 (1980).

[62] A. Girschik, F. Libisch, and S. Rotter, Phys. Rev. B **88**, 014201 (2013).

[63] Y. Fu, J. H. Wilson, and J. H. Pixley, Phys. Rev. B **104**, L041106 (2021).

[64] R. Chen, D.-H. Xu, and B. Zhou, Phys. Rev. B **100**, 115311 (2019).

[65] R. Chen, C.-Z. Chen, J.-H. Sun, B. Zhou, and D.-H. Xu, Phys. Rev. B **97**, 235109 (2018).

[66] J. Biddle, D. J. Priour, B. Wang, and S. Das Sarma, Phys. Rev. B **83**, 075105 (2011).

[67] R. Modak and S. Mukerjee, Phys. Rev. Lett. **115**, 230401 (2015).

[68] R. Modak and T. Nag, Phys. Rev. Research **2**, 012074(R) (2020).

[69] X. Deng, S. Ray, S. Sinha, G. V. Shlyapnikov, and L. Santos, Phys. Rev. Lett. **123**, 025301 (2019).

[70] H. Yao, H. Khoudli, L. Bresque, and L. Sanchez-Palencia, Phys. Rev. Lett. **123**, 070405 (2019).

[71] T. Liu, X. Xia, S. Longhi, and L. Sanchez-Palencia, SciPost Phys. **12**, 027 (2022).

[72] J. Wang, B. Lian, and S.-C. Zhang, Phys. Rev. Lett. **115**, 036805 (2015).
[73] R. Landauer, Philos. Mag. **21**, 863 (1970).
[74] M. Büttiker, Phys. Rev. B **38**, 9375 (1988).
[75] S. Rotter, J.-Z. Tang, L. Wirtz, J. Trost, and J. Burgdörfer, Phys. Rev. B **62**, 1950 (2000).
[76] S. Rotter, B. Weingartner, N. Rohringer, and J. Burgdörfer, Phys. Rev. B **68**, 165302 (2003).
[77] F. Libisch, S. Rotter, and J. Burgdörfer, New J. Phys. **14**, 123006 (2012).
[78] R. Zimmermann and C. Schindler, Phys. Rev. B **80**, 144202 (2009).
[79] See Supplemental Material at http://link.aps.org/supplemental/10.1103/PhysRevB.106.045417 for the details on the QSHI models, reservoir effect, connection between phase diagrams and band structures, normalized participation ratio, Born approximation for the continuum and lattice models.
[80] Chu. Rui-Lin, L. Jie, and S. Shun-Qing, Europhys. Lett. **100**, 17013 (2012).
[81] K. Hashimoto, C. Sohrmann, J. Wiebe, T. Inaoka, F. Meier, Y. Hirayama, R. A. Römer, R. Wiesendanger, and M. Morgenstern, Phys. Rev. Lett. **101**, 256802 (2008).
[82] B. Huckestein, Rev. Mod. Phys. **67**, 357 (1995).
[83] Y. Tokura, K. Yasuda, and A. Tsukazaki, Nat. Rev. Phys. **1**, 126 (2019).
[84] R. Watanabe, R. Yoshimi, M. Kawamura, M. Mogi, A. Tsukazaki, X. Yu, K. Nakajima, K. S. Takahashi, M. Kawasaki, and Y. Tokura, Appl. Phys. Lett. **115**, 102403 (2019).
[85] Y. Satake, J. Shiogai, G. P. Mazur, S. Kimura, S. Awaji, K. Fujiwara, T. Nojima, K. Nomura, S. Souma, T. Sato, T. Dietl, and A. Tsukazaki, Phys. Rev. Materials **4**, 044202 (2020).
[86] B. Béri and N. R. Cooper, Phys. Rev. Lett. **107**, 145301 (2011).
[87] M. Aidelsburger, M. Atala, M. Lohse, J. T. Barreiro, B. Paredes, and I. Bloch, Phys. Rev. Lett. **111**, 185301 (2013).
[88] M. Atala, M. Aidelsburger, M. Lohse, J. T. Barreiro, B. Paredes, and I. Bloch, Nat. Phys. **10**, 588 (2014).
[89] M. Aidelsburger, M. Lohse, C. Schweizer, M. Atala, J. T. Barreiro, S. Nascimbène, N. Cooper, I. Bloch, and N. Goldman, Nat. Phys. **11**, 162 (2015).
[90] G. Jotzu, M. Messer, R. Desbuquois, M. Lebrat, T. Uehlinger, D. Greif, and T. Esslinger, Nature (London) **515**, 237 (2014).
[91] N. Fläschner, B. Rem, M. Tarnowski, D. Vogel, D.-S. Lühmann, K. Sengstock, and C. Weitenberg, Science **352**, 1091 (2016).
[92] W. P. Su, J. R. Schrieffer, and A. J. Heeger, Phys. Rev. Lett. **42**, 1698 (1979).
[93] M. Atala, M. Aidelsburger, J. T. Barreiro, D. Abanin, T. Kitagawa, E. Demler, and I. Bloch, Nat. Phys. **9**, 795 (2013).
[94] L. Guidoni, C. Triché, P. Verkerk, and G. Grynberg, Phys. Rev. Lett. **79**, 3363 (1997).
[95] G. Roati, C. DErrico, L. Fallani, M. Fattori, C. Fort, M. Zaccanti, G. Modugno, M. Modugno, and M. Inguscio, Nature (London) **453**, 895 (2008).
[96] J. Billy, V. Josse, Z. Zuo, A. Bernard, B. Hambrecht, P. Lugan, D. Clément, L. Sanchez-Palencia, P. Bouyer, and A. Aspect, Nature (London) **453**, 891 (2008).
[97] J. E. Lye, L. Fallani, M. Modugno, D. S. Wiersma, C. Fort, and M. Inguscio, Phys. Rev. Lett. **95**, 070401 (2005).